Atmos. Chem. Phys. Discuss., 9, 2933–2965, 2009
www.atmos-chem-phys-discuss.net/9/2933/2009/

Atmospheric Chemistry and Physics Discussions

This discussion paper is/has been under review for the journal *Atmospheric Chemistry and Physics (ACP)*. Please refer to the corresponding final paper in *ACP* if available.

A new physically-based quantification of isoprene and primary organic aerosol emissions from the world's oceans

B. Gantt, N. Meskhidze, and D. Kamykowski

North Carolina State University, Raleigh, North Carolina, USA

Received: 9 December 2008 – Accepted: 19 December 2008 – Published: 29 January 2009

Correspondence to: N. Meskhidze (nmeskhidze@ncsu.edu)

Published by Copernicus Publications on behalf of the European Geosciences Union.

Abstract

The global marine sources of organic carbon (OC) are estimated here using a physically-based parameterization for the emission of marine isoprene and primary organic matter. The model developed in this study allowed us, for the first time, to explore the relative contributions of sub- and super-micron organic matter and phytoplankton-produced secondary organic aerosol (SOA) to the total OC fraction of marine aerosol. New laboratory measurements of isoprene production by some of the main phytoplankton species under a range of environmental conditions was scaled up, with the help of satellite products, to infer the total annual mean ocean isoprene emissions of 0.92 $\mathrm{Tg\,C\,yr^{-1}}$. The sensitivity studies using different schemes for the euphotic zone depth and ocean phytoplankton speciation produced the upper and the lower range of marine-isoprene emissions of 0.31 to 1.09 $\mathrm{Tg\,C\,yr^{-1}}$, respectively. Empirical relationships between fluxes of water soluble (WSOM) and water insoluble (WIOM) organic matter (OM) and chlorophyll-*a* concentration was used to estimate the total primary sources of oceanic sub- and super-micron OC of 1.26 and 19.01 $\mathrm{Tg\,C\,yr^{-1}}$, respectively. Using a fixed 3% mass yield for the conversion of isoprene to SOA, our model simulations show minor (less than 0.2%) contribution of ocean produced isoprene to the total marine source of OC. However, our model calculations also indicate that over the tropical waters, marine isoprene-derived SOA could contribute over 40% of the total monthly-averaged sub-micron OC fraction of marine aerosol. The estimated contribution of ocean-isoprene SOA to hourly averaged sub-micron marine OC fluxes is even higher, reaching nearly 100% over the vast regions of the oceans during the midday hours. As it is widely believed that cloud condensation nuclei (CCN) is typically dominated by sub-micron sized particles, our findings suggest that marine sources of SOA could play a critical role in modulating properties of shallow marine clouds and influencing the climate.

1 Introduction

Marine aerosols strongly affect properties and lifetime of stratiform clouds, influencing Earth's radiation budget and climate. Established sources of marine aerosol include primary emission of sea-salt particles and dimethylsulfide (DMS), the atmospheric oxidation of which is a major source of non-sea-salt (nss) sulfate in remote marine air (Shaw, 1983; Andreae et al., 1986; Charlson et al., 1987; O'Dowd et al., 1998). It has also been proposed that primary emissions of biogenic organic matter, bacterial and viral debris from wave breaking (Middlebrook et al., 1998; O'Dowd et al., 2004; Leck and Bigg, 2005) and secondary organic aerosol (SOA) from phytoplankton emitted biogenic volatile organic compounds (BVOCs) (O'Dowd et al., 2002; Meskhidze and Nenes, 2006; O'Dowd and de Leeuw, 2007) can act synergistically with the established mechanisms, leading to changes in marine aerosol chemical composition and number concentration. Significant abundances of organic carbon (OC) aerosols have been observed in marine environments (Novakov et al., 1997; Putaud et al., 2000; Cavalli et al., 2004; Yoon et al., 2007; Pio et al., 2007), particularly over the regions of enhanced oceanic biological activity (O'Dowd et al., 2004). Despite the significant progress in the recent decade, the mechanism and the magnitude of the marine OC sources are still highly uncertain, and the role of oceanic biota in modifying chemical composition and size distribution of marine cloud condensation nuclei (CCN) remains one of the most intriguing questions in the climate studies.

Marine organic aerosols appear to have two distinctly different sources and can be broadly classified as primary and secondary. Primary marine organic aerosols of biogenic origin are emitted from the ocean by the bubble bursting process, forming internally mixed aerosol of sea salt and organics (Middlebrook et al., 1998; Cavalli et al., 2004). Primary marine organic aerosols, especially in the sub-micron diameter size range, are typically comprised of organic colloids and aggregates (Leck and Bigg, 2005; Facchini et al., 2008). Analyses of marine aerosol chemical composition show that during the periods of high ocean productivity, concentration of water insoluble or-

ganic aerosols in the accumulation mode increase by almost a factor of 10 (from 0.07 to 0.619 $\mu g\,m^{-3}$) and comprise up to 45% of the total sub-micron aerosol mass in the marine air (O'Dowd et al., 2004).

Secondary organic aerosols of marine origin can be formed by the oxidation of phytoplankton-emitted biogenic volatile organic compounds (BVOCs). Out of many different phytoplankton-emitted BVOCs (e.g., DMS, halocarbons, and several types of non-methane hydrocarbons (NMHC) (Shaw et al., 1983; Bonsang et al., 1988; Tokarczyk et al., 1994), in this study we focus on oceanic fluxes of isoprene. Photooxidation of isoprene has been shown to lead to the formation of SOA (Claeys et al., 2004). Recent laboratory chamber studies show that SOA yields (defined as the ratio of the mass of SOA formed to the mass of isoprene reacted) are 1–2% at high NO_x levels (Kroll et al., 2005), ~3% at low NO_x levels (Kroll et al., 2006) and up to 24% from the reaction of isoprene with the nitrate radicals (Ng et al., 2008). Aqueous phase chemical processes offer additional SOA production pathways increasing the SOA yields up to 42% (Ervens et al., 2008). Further uncertainties in the assessments of global marine SOA sources arise from the fact that marine isoprene emissions have been shown to be sensitive to light (Lewis et al., 2001; Shaw et al., 2003; Liakakou et al., 2007; Sinha et al., 2007), temperature (Shaw et al., 2003) and species of phytoplankton (Shaw et al., 2003). The current estimates for global marine-source isoprene emissions range between 0.1–1.68 $Tg\,C\,yr^{-1}$ (Bonsang et al., 1992; Milne et al., 1995; Broadgate et al., 1997; Baker et al., 2000; Matsunaga et al., 2002; Palmer and Shaw, 2005; Sinha et al., 2007; Arnold et al., 2008) and are summarized in Table 1.

Modeling studies have demonstrated that the inclusion of marine organic aerosols decreases cloud droplet effective radii, increases droplet number concentration and results in better agreement with the measurements (Roelofs, 2008). Despite some recent advances in global marine organic aerosol emission estimates (Spracklen et al., 2008), treatment of phytoplankton-emitted isoprene, and therefore oceanic sources of SOA, is rather limited. In this study, we use new laboratory measurements of isoprene production by phytoplankton under a range of light conditions, as well as ocean surface

wind and chlorophyll-*a* concentration ([Chl-*a*])-dependent emissions of marine primary organic aerosols to create global maps of oceanic OC aerosol emissions.

2 Methods

2.1 Phytoplankton cultures and chlorophyll analysis

Three diatom strains *Thalassiosira weissflogii* (CCMP 1336), *Thalassiosira pseudonana* (CCMP 1335), and *Chaetoceros neogracile* (CCMP 1318), and a coccolithophore *Emiliania huxleyi* (CCMP 375) were grown on L1-based (Sigma-Aldrich) medium in a climate-controlled room with constant temperature and light conditions of 22°C and ~90 μE m^{-2} s^{-1} respectively. The seawater and nutrients were prepared for culturing by autoclaving overnight to remove bacterial contamination. Cultures were grown in 1 liter Erlenmeyer flasks covered with aluminum foil allowing air transfered to prevent carbon dioxide limitation. Prior to the experiment, 20 ml samples were transfer onto Whatman GF/F filters under vacuum and stored in freezer for later analysis of [Chl-*a*]. Chlorophyll-*a* was extracted with 90% acetone and concentration determined following the method of Holm-Hansen and Riemann (1978) using a Turner fluorometer model #450.

2.2 Isoprene measurements

After an incubation period ranging from 7–14 days, 30 ml aliquots of the dense phytoplankton populations cultures were transferred to Wheaton 40 ml EPA glass vials and sealed using open-top screw caps with 10 mm TFE and 90 mm silicone septa. The 10 ml of headspace remaining above the sample maximized concentrations of isoprene emitted by the phytoplankton while ensuring that CO_2 limitation did not occur during the experiment. To assess the effect of changing incoming solar radiation for isoprene production, the phytoplankton were exposed to various levels of light intensity ranging from 0 to 1200 μE m^{-2} s^{-1} (~0 to 600 W m^{-2}) for up to eight hours under

ACPD
9, 2933–2965, 2009

a constant temperature of 23°C controlled by a Neslab CFT-33 Refrigerated Recirculator (Thermo Fisher Scientific, Waltham, MA). The samples were suspended over 6 halogen lights (Philips 250W Projector Lamp #13095) in a water bath with circulating water to absorb heat from the lights. Irradiance inside the water bath was measured by QSL-100 Laboratory Quantum Scalar Irradiance Meter (Biospherical Instruments, San Diego, CA). The intensity of light reaching the samples was controlled by lining the bottom of the water bath with several layers of semi-translucent fiberglass screen. Prior calibration testing revealed that each layer of the screen absorbed approximately half of the incoming light.

Laboratory measurements of isoprene concentrations were taken using a headspace gas chromatography (GC) with a Photovac Voyager (Photovac, Inc., Waltham, MA) portable GC with a photoionization detector (PID). Ultra high-purity nitrogen was used as a carrier gas. The system was calibrated against a standard containing 103.2 ± 10.3 ppb (v/v) isoprene in ultrapure nitrogen (Scott-Marrin Inc., Riverside, CA). The detector output is linear from 0 to 460 ppb v/v isoprene concentration with an intercept through zero (Geron et al., 2006). We estimate that both precision and accuracy were within 10% as determined by repeated measurements of the standard gas and inter-calibration against PTR-MS (Proton Transfer Reaction Mass Spectrometry) during intensive field study at the University of Virginia at Charlottesville. According to the instrument calibration records carried out at Photovac, Inc., the lower detection limit of our analytical system is 3 ppbv. Using a Hamilton Gastight #1750 syringe, 500 μL of the headspace from each sample were injected in the gas sample loop with 0.5 to 1 h intervals to monitor the changes in isoprene concentrations inside the sealed vials. Column temperature was isothermal at 60°C and pressure was constant at 6 psi. During each experiment, we kept several phytoplankton samples in the dark and observed isoprene concentration levels that were below the detection limit. This indicates that like *Prochlorococcus* (Shaw et al., 2003), isoprene production from diatom and coccolithophore species were negligible under nighttime conditions. The isoprene concentrations from the headspace of blank seawater samples were measured and used as the

background air that was subtracted from the phytoplankton sample measurements.

Figure 1 shows that for all types of phytoplankton, production rates increase under increasing light intensity with a rapid increases at low levels and gradual increases at high levels of irradiance, in a pattern similar to terrestrial plants (Guenther et al., 1993). These measurements were fit to a logarithmic curve with diatoms having the highest isoprene production and coccolithophores having the lowest. Amongst the diatoms, *C. neogracile* had the highest isoprene production under all light conditions, followed by *T. weissflogii* and *T. pseudonana* with similar production rates. Symbols on Fig. 1 show the average of all measurements for a given light intensity and the error bars indicate the highest and the lowest measured values. A wide range in emission rates is likely to be attributed to expected photoinhibition of marine phytoplankton photosynthesis (Platt et al., 1980) and the different growth conditions of planktonic species. Although results were inconclusive, it was also noticed, that for a given [Chl-*a*], "young" plankton exhibited somewhat higher isoprene emission rates compared to the "old" ones. In addition, differences in emission rates were noticed when different amounts of nutrients were used for the plankton growth. The isoprene production rates P (μmole isoprene (gram chlorophyll-*a*)$^{-1}$ h^{-1}) are given by the equation:

$$P = EF * \ln I^2 \quad (1)$$

where EF is the emission factor for each phytoplankton species (0.042 for diatoms, 0.032 for *Prochlorococcus*, 0.029 for *Synechococcus*, 0.019 for coccolithophores, and 0.028 for other phytoplankton) and I is the ambient light intensity (μE m^{-2} s^{-1}). We calculated the emission factors for diatoms and coccolithophores by fitting a logarithmic curve to our measurements, and approximated the emission factors for *Prochlorococcus*, *Synechococcus*, and others by converting the daily isoprene production rates from Shaw et al. (2003) to hourly rates and using a similar logarithmic curve to extrapolate measurements taken at 90 μE m^{-2} s^{-1} to light intensities greater than 1200 μE m^{-2} s^{-1}.

2.3 Phytoplankton speciation

Global phytoplankton speciation is estimated by using two distinct methods: the PHYSAT (Alvain et al., 2005), and the nutrient depleting temperature (NDT) (Kamykowski et al., 2002). In the PHYSAT method, satellite-derived normalized water-leaving radiances (nLw) from 5 different wavelengths are compared to the lookup tables of average nLw (nLw*) for each wavelength based on [Chl-*a*]. Speciation is determined based on the unique effects on satellite-observed nLw by the pigments of each phytoplankton class. The global monthly maps of nLw data at 1° latitude × 1° longitude resolution were created by regridding the Sea-viewing Wide Field-of-view Sensor (SeaWiFS) monthly-averaged ~9 km resolution nLw data for the year 2001. By comparing the obtained nLw data with the lookup tables of nLw*, the following dominant phytoplankton classes were identified: *Nanoeukaryotes*, *Prochlorococcus*, *Synechococcus*, diatoms, and phaeocystis-like plankton/coccolithophores. In the NDT method, seasonal and inter-annual nutrient (i.e., nitrate, phosphate, silicate and iron) variability and remotely sensed [Chl-*a*] data is used to infer the likely phytoplankton cell size and taxonomic composition (Kamykowski et al., 2002). SeaWiFS monthly-averaged ~9 km resolution sea surface temperature (SST) was regridded to 1°×1° and compared to NDT tables of nutrient categories (Kamykowski et al., 2002) to create global monthly maps of phytoplankton classes for year 2001. The two methods (i.e., PHYSAT and NDT) show similar spatial and seasonal distribution of plankton speciation (not shown) and are in general agreement with the outputs from the NASA Ocean Biochemical Model (NOBM) (Gregg et al., 2003). Both PHYSAT and NDT models place diatoms in the high latitude oceans above 40° North or South and upwelling regions, coccolithophores in the polar regions, and *Prochlorococcus*/*Synechococcus* in the ocean gyres and equatorial regions. In this study, the PHYSAT model is used as a default for the assessments of the global marine-isoprene emissions. In Sect. 4.1 we present sensitivity calculations using NDT method to estimate how distinct methods and the uncertainties in phytoplankton community composition can affect our results for total

ACPD
9, 2933–2965, 2009

global oceanic emissions of isoprene.

2.4 Oceanic isoprene emissions

Estimated isoprene emission rates for some of the major phytoplankton species under variable light intensity were used to create global maps of oceanic isoprene emission. Photosythetically active radiation (PAR) measurements (μE m^{-2} s^{-1}) were converted to total solar radiation (W m^{-2}) by using the following approximate conversion 2 μE m^{-2} s^{-1}=1 W m^{-2} (Jacovides et al., 2004). Surface [Chl-*a*] (mg m^{-3}) was derived from monthly-averaged ~9 km, Level 3 SeaWiFS satellite data regridded to 1°×1°. SeaWiFS was shown to have the most accurate retrieval of surface [Chl-*a*] in coastal as well as remote oceanic sites (Blondeau-Patissier et al., 2004). The amount of solar radiation received by phytoplankton at different depths of the water column is calculated using hourly 1°×1° all-sky surface incoming solar radiation I_o (W m^{-2}) from the Global Weather Research and Forecasting Model (G-WRF) v. 3.0 (Richardson et al., 2007). The values of downwelling irradiance within a water column were characterized using the diffuse attenuation coefficient values at 490 nm $k_d(490)$ (m^{-1}) from regridded SeaWiFS data (O'Reilly et al., 1998). The light propagation throughout the water column with depth d (meters) is estimated by applying Beer-Lambert's Law, given by: $I = I_o\, e^{-k_d(490)d}$. The total water depth D_w through which isoprene production can occur in our model was assumed to extend from the surface to the point at which the light levels are reduced to 2.5 W m^{-2}, which is the level at which the photosynthesis ceases in *Prochlorococcus* (Shaw et al., 2003). This depth, which represents the maximum possible extent of the planktonic euphotic zone, is determined using the following equation:

$$D_w = \left(-\ln\left(\frac{2.5}{I_o}\right) * k_d(490)^{-1}\right) \quad (2)$$

In this formulation it is assumed that the light at depth will continue to diffuse at a rate identical to the surface diffuse attenuation retrieved by SeaWiFS. Calculations

documenting the sensitivity of our global marine-isoprene fluxes to selection of the ocean euphotic zone depth are presented in Sect. 4.2.

The total column isoprene emission E (μmole h^{-1}) is found by integrating Eq. (1) by D_w:

$$E = SA * D_w * [\text{Chl-}a] * F * \int_0^{D_w} P \, \partial d \quad (3)$$

here SA is the surface area of the 1°×1° grid cell (m^2) and F is the emission fraction (i.e., fraction of water column produced isoprene emitted to the atmosphere). The emission fraction is calculated as the ratio of sea-air flux of isoprene to total isoprene loss in the water column from chemical, biological, and ocean-air exchange following the method of Palmer and Shaw (2005).

2.5 Primary organic aerosol emissions

Chemical analyses of marine aerosols show that OC that resides in sub- and super-micron modes of sea-spray particles has considerably different water solubility (Facchini et al., 2008). While water insoluble organic carbon (WIOC) comprises the major portion (94±4%) of sub-micron OC particles, water soluble organic carbon (WSOC) contributes more than one-third (33±3%) of total carbon in the coarse size fraction of marine aerosols (Facchini et al., 2008). Here the global marine primary OC emissions are estimated separately in sub- and super-micron range. Over the productive regions of the oceans, the sub-micron range marine aerosol mass was shown to be dominated by insoluble organics, while the super-micron size range aerosols were dominated by sea-salt (Facchini et al., 2008). The sub-micron mass flux F_{sub} (ng m^{-2} s^{-1}) of marine primary organic aerosols can be parameterized by multiplying the sea-spray emission rates of particles less than 1 μm diameter by the water insoluble organic fraction of sub-micron marine aerosols (Ceburnis et al., 2008; Langmann et al., 2008):

$$F_{\text{sub}} = 4.72 * 10^{-5} * U_{22}^{4.22} * [\text{Chl-}a] \quad (4)$$

where U_{22} is the wind speed at 22 m above the water surface (m s^{-1}). We estimate U_{22} using 4-times daily 10 m wind velocity from the National Center for Environmental Prediction (NCEP) Reanalysis (http://www.cdc.noaa.gov/cdc/reanalysis/) for the year 2001. The wind data, originally in a T62 Gaussian grid, was spatially interpolated to the $1^{\circ} \times 1^{\circ}$ grid and converted to 22 m winds by applying the correction factor from Andreas (1998). For simplicity, we assume neutral stability and implement a logarithmic wind profile with the height. The WIOM flux was converted to an OC flux by using the OC to WIOM conversion factor of 1.4 (Decesari et al., 2007; Facchini et al., 2008).

The super-micron primary organic aerosol mass flux is calculated in a way similar to the sub-micron flux, though using a different sea-spray function and an organic percent of the sea-spray, reflecting the minor contribution of organics to the coarse aerosol mode. The sea-spray number flux from Smith and Harrison (1998) was converted into a mass flux by assuming spherical particles with a density of sea-salt (2.165 g cm^{-3}). The mass flux was integrated for particles with diameters from 1–8 μm, corresponding to the size range of super-micron particles measured in most marine aerosol studies (O'Dowd et al., 2007). Despite the dominance of sea-salt in super-micron marine aerosols, it was shown that over the productive region of the Northern Atlantic Ocean, organic mass contributed ~3% of 4–8 μm diameter sea-spray particle mass (Facchini et al., 2008). The super-micron mass flux F_{super} (ng m^{-2} s^{-1}) of marine primary organic aerosols is parameterized as:

$$F_{super} = (6.86 * 10^{-5} * U_{10}^{3.5} + 1.75 * 10^{-4} * U_{10}^{3}) * [\text{Chl-}a] \quad (5)$$

where U_{10} is the wind speed at 10 m above the water surface, obtained from the spatially-interpolated 10 m NCEP 4-times daily wind velocity datasets. The super-micron mass flux of marine primary OC was calculated using OC to OM conversion factor of 1.52 reflecting the higher WSOC content of coarse marine organic aerosols (Decesari et al., 2007; Facchini et al., 2008).

3 Results

Recent studies suggest that strong physico-chemical properties of marine aerosols can be linked to the observed seasonal cycle of [Chl-*a*] in ocean surface waters (Yoon et al., 2007). Based on the vertical concentration gradient measurements of marine aerosols at the coastal research station in Mace Head, Ireland, two distinct production mechanisms for WSOC and WIOC organic carbon were proposed (Ceburnis et al., 2008). It was shown that WIOC had a net production at the surface (i.e., primary production), while WSOC was predominantly of secondary origin. In order to derive global oceanic source of OC, we consider separately primary and secondary organic aerosol emissions.

3.1 Global isoprene emissions

Global production of SOA of marine origin is calculated here based on global sea-air isoprene fluxes assuming 3% mass yield of isoprene to SOA (Henze and Seinfeld, 2006). Figures 2a,b show the seasonal changes in spatial distribution of isoprene emissions for the year 2001. Fluxes range from $\sim 5 \times 10^5$ to 6×10^8 molecules cm^{-2} s^{-1}, which are comparable with published in-situ flux measurements and modeling results (Bonsang et al., 1992; Milne et al., 1995; Broadgate et al., 1997; Baker et al., 2000; Matsunaga et al., 2002; Broadgate et al., 2004; Greenburg et al., 2005; Liakakou et al., 2007; Sinha et al., 2007). Figure 2 shows that the highest emission values are generally estimated during the spring and summer seasons (September–March in the Southern Oceans and April–August in the Northern Oceans); coastal waters affected by upwelling and river runoffs also demonstrate elevated emission rates. Overall, the emission pattern of Fig. 2 is similar to that for [Chl-*a*] with large values typically observed in regions with the adequate light and nutrient availability (e.g., coastal margins and upwelling regions) and low concentrations in the gyres (see Auxiliary material Fig. S1: http://www.atmos-chem-phys-discuss.net/9/2933/2009/acpd-9-2933-2009-supplement.pdf). However, careful inspection of Fig. 2

shows some considerable differences between the surface [Chl-*a*] and isoprene emission rates. Despite low chlorophyll abundance, widespread areas in equatorial marine regions have moderately high isoprene emission rates often reaching more than 6×10^7 molecules cm^{-2} s^{-1}. Such high emission rates throughout the year are likely to be attributed to the elevated solar radiation levels. Elevated rates of emissions and water concentrations of isoprene and other NMHC have been observed in several locations in equatorial waters, presumably because of the high solar radiation (Bonsang et al., 1988).

In addition to monthly mean flux values, diurnal variations in isoprene emission rates were also simulated using hourly incoming surface solar radiation values from the G-WRF model. When considering global marine sources of SOA it is very important for the models to correctly capture the diurnal variations of marine isoprene emissions. Due to the light dependence of isoprene production, it was shown that maximum midday emissions of phytoplankton-produced isoprene are roughly an order of magnitude higher compared to the nighttime emissions (Lewis et al., 2001; Liakakou et al., 2007; Sinha et al., 2007). Furthermore, the effects of marine isoprene-derived SOA on properties of shallow marine clouds and the resulting changes in short-wave radiative flux at the top of the atmosphere are likely to be the most pronounced during the daylight conditions (Meskhidze and Nenes, 2006). Therefore, calculating isoprene emissions on a frequency of an hour or less will provide better estimates for the possible contribution of SOA to marine OC aerosol composition. Currently there are very few studies reporting the diurnal variations of in-situ measurements of marine isoprene emissions. In Fig. 3a, the simulated isoprene emissions from the North Pacific Ocean between 19 May and 26 May 2001 are compared to in-situ measurements from Matsunaga et al. (2002) from the same period and location. Figure 3a shows that in general, modeled emission rates are comparable to the observations in both magnitude and diurnal variation. However, the figure also shows the small overestimation of oceanic isoprene emissions during the day and strong underestimations at night. Such differences between the simulated and observed emissions should be attributed to the absence of

isoprene accumulation in the modeled water column.

Figure 3b shows the simulated isoprene emissions near Raunefjord, Norway from May 31 to July 10, 2001. Compared to in-situ measurements of Sinha et al. (2007) conducted during the same time period but in year 2005, our emission rates are lower by a factor of 2–3. Sinha et al. (2007) reported a mean isoprene flux value of 0.12 ng m^{-2} s^{-1} and daily maximum flux values ranging from ~0.2 to 0.9 ng m^{-2} s^{-1}. The most likely reason for the discrepancy between the simulated and observed fluxes is the lower chlorophyll-*a* content of our 2001 grid, which had a [Chl-*a*] of 0.84 mg m^{-3} compared to the reported [Chl-*a*] of ~2.0 mg m^{-3} by Sinha et al. (2007). Despite the fact that isoprene emissions from phytoplankton do not scale linearly with the surface chlorophyll concentration, lower [Chl-*a*] is believed to be the major factor for such differences in the emissions. Other factors may include differences in the dominant phytoplankton classes present at the same locations during the two different time periods and the 1°×1° grid-cell smoothing of elevated, but localized, emissions. Overall, Fig. 3a, b demonstrate that despite some difficulties with the total emission rates, the model was capable of capturing the diurnal cycle in marine isoprene emissions.

In this study we estimate the total global sea-air isoprene flux to be ~0.92 Tg C yr^{-1}. This value is within the range of estimates of 0.19–1.68 Tg C yr^{-1} proposed by previous studies based on in-situ measurements (Milne et al., 1995; Bonsang et al., 1992; Broadgate et al., 1997) and satellite observations (Palmer and Shaw, 2005; Arnold et al., 2008). Sensitivity calculations for different plankton speciation and water column depths presented in Sect. 4 show an estimated range of global isoprene emissions between 0.31 and 1.09 Tg C yr^{-1}.

3.2 Global primary organic aerosol emissions

The sub-micron primary OC emission rates for January and July, 2001 are shown in Fig. 4a, b. These figures show that the areas in the mid-latitudes from about 40° to 60° North or South of the equator have high emission rates throughout the year. In these regions primary OC emissions are mainly controlled by high surface ocean

winds, so emission rates in excess of 10^{10} molecules C cm^{-2} s^{-1} are common. The lowest primary OC emission rates occur near the equatorial regions resulting from the relatively low surface wind speed and [Chl-*a*] (see Fig. 4). The global distribution of super-micron primary organic aerosol emission rates, (Fig. 4c, d) are similar to the sub-micron fluxes but with higher values owing to the higher mass of larger particles. In this study we estimate global annual ocean emissions for sub- and super-micron primary OC to be about 1.3 and 19 Tg C yr^{-1}, respectively. Different estimates for the global marine OC emissions are summarized in Table 1.

3.3 Relative importance of primary and secondary organic aerosols of marine origin

The relative contribution of ocean emitted primary organic aerosols and phytoplankton-produced SOA to the total marine OC aerosol burden has been a topic of discussion in several recent papers (Vaattovaara et al., 2006; O'Dowd et al., 2007; Arnold et al., 2008). Prognostic, physically-based emission mechanisms for both primary and secondary marine organic aerosols developed in this study allow us to evaluate spatial and temporal distribution of the percent contribution of phytoplankton-derived SOA to the total simulated marine organic aerosol emissions. Here we mainly focus on sub-micron primary marine organic aerosol and on phytoplankton-derived SOA, since it is believed that they are the main contributors to water soluble and water insoluble organic fraction of marine aerosol, influencing their CCN activation potential (Nenes et al., 2002; O'Dowd et al., 2004). In order to compare isoprene-derived SOA emission rates to that of sub-micron primary OC aerosols, we assume OC to SOA conversion factor of 1.6 (Turpin et al., 2001). Figure 5a, b show widespread areas of the equatorial oceans where SOA from phytoplankton-emitted isoprene contributes over 40% of total monthly averaged OC mass fraction of sub-micron marine aerosols. This figure also shows that despite larger ocean fluxes of isoprene in productive regions of the North Atlantic, North Pacific and the Southern Oceans (see Fig. 2), monthly averaged marine SOA contributes minor fraction of total sub-micron ocean-emitted OC in these polar waters.

Figure 6 shows that the zonally-averaged emission rates of phytoplankton-produced SOA are comparable to sub-micron primary OC aerosols in equatorial regions, while in most other locations, marine sources of OC are dominated by sub-micron primary aerosols. Such high sea-air flux values of sub-micron primary OC (more than an order of magnitude higher than the emission rates for marine-source SOA) is primarily due to the year round elevated wind speed in the high latitude regions. Overall, despite phytoplankton-produced SOA being a minor contributor to the global sub-micron marine aerosol OC fraction (see Table 1), Figs. 5 and 6 show that marine-source SOA may have considerable effect on CCN composition over vast regions of the oceans.

In addition to large spatial differences, ocean emissions of BVOCs are also characterized by strong diurnal variations (Bonsang et al., 1988; Sinha et al., 2007). Therefore, using global monthly averaged values for phytoplankton-emitted isoprene may significantly underestimate the contribution of marine SOA to the total organic fraction of ocean emitted aerosols during the day and overestimate at night. The contribution from daily maximum marine isoprene-derived SOA to the organic fraction of marine CCN is further explored on Fig. 7. The global maps of Fig. 7 can be interpreted as an hourly averaged "snapshot" for the potential impact of midday SOA emissions on total (primary and secondary) sub-micron marine OC flux. Figure 7 shows that the localized percent contributions of marine isoprene-derived SOA to the total sub-micron marine OC emissions approach 100%, even in areas with low monthly averaged values (i.e., polar waters). Therefore, Fig. 7 highlights the need for improved assessments of the marine isoprene emissions in different parts of the global ocean. It also shows that a marine isoprene emission time step on the order of an hour may be required for the global models to correctly capture the contribution of ocean-derived SOA to water soluble and water insoluble OC fraction of marine CCN.

3.4 Sensitivity analyses

In this section, sensitivity calculations are presented to illustrate how reasonable variations in some of the key model parameters affect the total global emissions of

phytoplankton-produced isoprene. Specifically we address the model sensitivities to phytoplankton speciation and the extent of the water column through which the isoprene production occurs.

3.5 Phytoplankton speciation

Two different phytoplankton speciation schemes implemented in this study allow us to examine the impact on marine-source isoprene emission estimates to the uncertainties in the plankton speciation. The primary difference in speciation between the two examined methods (i.e., PHYSAT and NDT) is the diatom dominance in larger areas of high latitude oceans. Because diatoms produce isoprene at a rate that is roughly 30% higher than other phytoplankton classes, the NDT speciation method gives somewhat greater high latitude isoprene emissions and increases the estimate of total global annual isoprene fluxes to 1.09 Tg C yr^{-1}, i.e., ~20% higher than the PHYSAT estimate. This finding suggests that differences in phytoplankton speciation (deduced using two distinct methods based on remotely-sensed data) are likely to contribute 20% uncertainty in global isoprene emissions. This result also points to the uncertain nature of estimating isoprene emissions using remotely-sensed data and highlights the need for supplementary in-situ measurements of phytoplankton speciation in different parts of the global ocean.

3.6 Variable euphotic depth

For a sensitivity analysis of the effect of euphotic zone estimate on marine-isoprene production, we set D_w to one optically-sensed depth given as: $D_w = k_d(490)^{-1}$. When limiting isoprene production to only the first optical depth (~1m to ~50m based on the surface ocean [Chl-*a*]), the total global annual ocean isoprene emission are reduced to 0.31 Tg C yr^{-1}. This estimate should be considered as the low limit of isoprene emissions, since it is not uncommon for the seawater [Chl-*a*] and dissolved isoprene maximum to occur in the mixed layer well below the first optical depth viewable by the

satellites (Milne et al., 1994).

4 Conclusions

A physically-based parameterization for the emission of marine isoprene and primary organic matter was developed and used to estimate the global oceanic sources of OC. In this study new laboratory measurements of isoprene production by different phytoplankton species under a range of light conditions with a light intensity reaching 1200 μEm^{-2} s^{-1} were preformed. The obtained relationship was used in conjunction with remotely sensed data of [Chl-*a*], phytoplankton speciation and water-attenuation of solar downwelling irradiance to simulate, for the first time, the diurnal variation of marine isoprene production in different parts of the global ocean. We estimate the total mean global marine-source isoprene emission to be 0.92 Tg C yr^{-1}. Based on the sensitivity studies using different schemes for the euphotic zone depth and ocean phytoplankton speciation, we propose the upper and the lower range of marine-isoprene emissions to be between 0.31 and 1.09 Tg C yr^{-1}, respectively. In agreement with the in-situ studies, our simulations show very large differences between daytime and nighttime emissions of marine isoprene. Such large diurnal variation in isoprene production rates could partially reconcile considerable discrepancies in past global marine isoprene production estimates. Despite comparable results, differences remain between observed and our model-predicted marine isoprene fluxes, mainly under nighttime conditions. Underprediction of nighttime emissions of marine isoprene in our model is likely to be attributed to the absence of isoprene accumulation mechanism in the water column.

The model developed in this study allowed us to explore the relative contribution of sub- and super-micron organic matter and phytoplankton-derived SOA to the total OC fraction of marine aerosol. To do so, marine isoprene emissions were converted into an SOA fluxes using a fixed 3% mass yield. Our model simulations show that phytoplankton-derived isoprene is a minor source of a total global annually emitted marine OC aerosol. The estimated range for oceanic SOA represents minor fraction

of 20.3 Tg C yr^{-1} of total ocean-emitted OC. However, the importance of marine secondary organic aerosols becomes apparent, when phytoplankton derived SOA is compared to sub-micron primary marine organic aerosol emissions. Sub-micron fraction was chosen for the comparison since it is believed that sub-micron OC influences the CCN activation potential of marine aerosols. Our model simulations show that monthly averaged marine sub-micron primary OC emissions are considerably higher than that of isoprene-derived SOA in most oceanic regions, except in tropical waters, where marine isoprene-derived SOA contributes more than 40% of the total sub-micron OC fraction of marine aerosol. When hourly isoprene emission values are used, simulations show even larger contribution from phytoplankton-derived SOA. During the midday hours, typically associated with the largest production of isoprene, marine-source SOA can contribute up to 100% of total sub-micron OC fraction of marine CCN over vast regions of the oceans. Since the effect of marine SOA is particularly pronounced during the daylight conditions, an isoprene emission time step on the order of an hour may be required for global models to correctly capture the climate implication of the oceanic secondary OC source.

Cooperative efforts of researchers for in-situ emission measurements of isoprene and other BVOCs over biologically active regions of remote oceans combined with the extensive laboratory-based experiments are needed to gain further insight into the production of isoprene and other BVOCs by marine biota and improve global estimates of marine BVOC fluxes. Work is also needed to better constrain speciation and column abundances of phytoplankton in estuaries and near coastal regions for the detailed, finer scale modeling of the near-coastal emission rates. Future studies should also focus on elucidation of the potential effects of nutrient limitation, bacterial population, and grazing pressure on the rates of marine isoprene production. Additional uncertainties in isoprene production rates, SOA yields, wind fields and the limited sets of observational data for the emissions of primary organic matter are all likely to affect our model predicted fluxes of primary and secondary marine OC aerosol. Despite these limitations, however, we believe that modeling results presented in this study demonstrate

that phytoplankton-produced SOA can significantly affect the sub-micron OC fraction of marine CCN.

Acknowledgements. This research was supported by the Office of Science (BER), US Department of Energy, Grant No. DE-FG02-08ER64508. The authors would like to thank Robert Reed of the NCSU Center for Applied Aquatic Ecology for his help with phytoplankton samples, Joshua Hemperly for his help with the Global WRF solar radiation data, Jose Fuentes and Stephen Chan at the University of Virginia for their help running samples using the PTR-MS, Severine Alvain for providing the PHYSAT nLw* lookup tables, and Vinayak Sinha for providing isoprene flux data.

References

Alvain, S., Moulin, C., Dandonneau, Y., and Breon, F. M.: Remote sensing of phytoplankton groups in case 1 waters from global SeaWiFS imagery, Deep-Sea Res. I, 52, 1989–2004, 2005.

Andreae, M. O., Charlson, R. J., Bruynseels, F., Storms, H., Grieken, R. V., and Maenhaut W. : Internal Mixture of Sea-salt, Silicates, and Excess Sulfate in Marine Aerosols, Science, 27, 232, 4758, 1620–1623, doi: 10.1126/science.232.4758.1620, 1986.

Andreas, E.: A New Sea Spray Generation Function for Wind Speeds up to 32 m s^{-1}, J. Phys. Oceanogr., 28, 2175–2184, 1998.

Arnold, S. R., Spracklen, D. V., Williams, J., Yassaa, N., Sciare, J., Bonsang, B., Gros, V., Peeken, I., Lewis, A. C., Alvain, S., and Moulin, C.: Evaluation of the global oceanic isoprene source and its impacts on marine organic carbon aerosol, Atmos. Chem. Phys. Discuss, 8, 16445-16471, 2008.

Baker, A. R., Turner, S. M., Broadgate, W. J., Thompson, A., McFiggans, G. B., Vesperini, O., Nightingale, P. D., Liss, P. S., and Jickells, T. D.: Distribution and sea-air fluxes of biogenic trace gases in the eastern Atlantic Ocean, Global Biogeochem. Cy., 14, 871–886, 2000.

Blondeau-Patissier, D., Tilstone, G. H., Martinez-Vicente, V., and Moore, G. F.: Comparison of bio-physical marine products from SeaWiFS, MODIS, and a bio-optical model with in-situ measurements from Northern European waters, J. Opt. A: Pure Appl. Opt., 6, 875–889, 2004.

Bonsang, B., Kanakidou, M., Lambert, G., and Monfray, P.: The marine source of C2-C6 aliphatic hydrocarbons, J. Atmos. Chem., 6, 3–20, 1988.
Bonsang, B., Polle, C., and Lambert, G.: Evidence for marine production of isoprene, Geophys. Res. Lett., 19, 1129–1132, 1992.
Broadgate, W. J., Liss, P. S., and Penkett, S. A.: Seasonal emissions of isoprene and other reactive hydrocarbon gases from the ocean, Geophys. Res. Lett., 24, 2675–2678, 1997.
Cavalli, F., Facchini, M. C., Decesari, S., Mircea, M., Emblicia, L., Fuzzi, S., Ceburnis, D., Yoon,Y. J., O'Dowd, C. D., Putaud, J.-P., and Dell'Acqua, A.: Advances in characterization of size resolved organic matter in marine aerosol over the North Atlantic, J. Geophys. Res., 109, D24215, doi:10.1029/2004JD005137, 2004.
Ceburins D., O'Dowd, C., Jennings, G. S., Facchini, M. C., Emblico, L., Decesari, S., Fuzzi, S., and Sakalys, J.: Marine aerosol chemistry gradients: Elucidating primary and secondary processes and fluxes, Geophys. Res. Let., 35, L07804, doi:10.1029/2008GL033462, 2008.
Charlson, R. J., Lovelock, J. E., Andreae, M. O., and Warren, S. G.: Oceanic phytoplankton, atmospheric sulfur, cloud albedo and climate, Nature, 326, 655–661, 1987.
Claeys, M.B., Graham, G., Vas, W., Wang, R., Vermeylen, V., Pashynska, Cafmeyer, J., Guyon, P., Andreae, M. O., Artaxo, P., and Maenhaut, W.: Formation of Secondary organic aerosols through photooxidation of isoprene, Science, 303, 1173–1176, 2004.
Decesari, S., Facchini, M. C., Mircea, M., Cavalli, F., Emblico, L., Fuzzi, S., Moretti, F., and Tagliavini, E.: Source attribution of water-soluble organic aerosol by nuclear magnetic resonance spectroscopy, Environ. Sci. Technol., 41, 2479–2484, 2007.
Edney E. O., Kleindienst, T. E., Jaoui, M., Lewandowski, M., Offenberg, J. H., Wang, W., Claeys, M.: Formation of 2-methyl tetrols and 2-methylglyceric acid in secondary organic aerosol from laboratory irradiated isoprene/NO_X/SO_2/air mixtures and their detection in ambient $PM_{2.5}$ samples collected in the eastern United States, Atmos. Environ., 39, 5281–5289, 2005.
Ervens B., Carlton, A. G., Turpin, B. J., Altieri, K. E., Kreidenweis. S. M., and Feingold, G.: Secondary organic aerosol yield from cloud-processing of isoprene oxidation products, Geophys. Res. Lett., 35, L02816, doi:10.1029/2007GL031828, 2008.
Facchini M. C., Rinaldi, M., Decesari, S., Carbone, C., Finessi, E., Mircea, M., Fuzzi, S., Ceburnis, D., Flanagan, E., Nilsson, D., Leeuw, G., Martino, M., Woeltjen J., and O'Dowd, C. D.: Primary sub-micron marine aerosol dominated by insoluble organic colloids and aggregates, Geophys. Res. Lett., 35, L17814, doi:10.1029/2008GL034210, 2008.

Geron, C., Guenther, A., Greenberg, J., Karl, T., and Rasmussen, R.: Biogenic volatile organic compound emissions from desert vegetation of the southwestern US, Atmos. Environ., 40, 1645–1660, 2006.
Guenther, A. B., Zimmerman, P. R., Harley, P. C., Monson, R. K., and Fall, R.: Isoprene and monoterpene emission rate variability: Model evaluations and sensitivity analyses, J. Geophys. Res., 98, 12609–12617, 1993.
Henze, D. K. and Seinfeld, J. H.: Global secondary organic aerosol from isoprene oxidation, Geophys. Res. Lett., 33, L09812, doi:10.1029/2006GL025976, 2006.
Holm-Hansen D. and Riemann B.: Chlorophyll-*a* determination: improvements in methods, Oikos, 30, 438–447, 1978.
Jacovides, C.P., Tymvios, F.S., Papaioannou, G., Asimakopoulos, D.N., and Theofilou, C.M.: Ratio of PAR to broadband solar radiation measured in Cyprus, Agric. Forest Meteorol., 121, 135–140, 2004.
Kamykowski, D., Zentara, S. J., Morrison, J. M., and Switzer, A. C.: Dynamic global patters of nitrate, phosphate, silicate, and iron availability and phytoplankton community composition from remotely sensing data, Global Biogeochem. Cy., 16, 4, 1077, doi:10.1029/2001GB001640, 2002.
Kroll, J. H., Ng, N. L., Murphy, S. M., Flagan, R. C., and Seinfeld, J. H.: Secondary organic aerosol formation from isoprene photooxidation, Environ. Sci. Technol., 40, 1869–1877, doi:10.1021/es0524301, 2006.
Langmann, B., Scannell, C., and O'Dowd, C.: New Directions: Organic matter contribution to marine aerosols and cloud condensation nuclei, Atmos. Environ., 42, 7821–7822, 2008.
Lewis, A. C., Carpenter, L. J. and Pilling, M. J.: Nonmethane hydrocarbons in Southern Ocean boundary layer air, J. Geophys. Res., 106, D5, 4987–4994, 2001.
Liakakou, E., Vrekoussis, M., Bonsang, B., Donousis, Ch., Kanakidou, M., and Mihalopoulos, N.: Isoprene above the Eastern Mediterranean: Seasonal variation and contribution to the oxidation capacity of the atmosphere, Atmos. Environ., 41, 1002–1010, 2007.
Matsunaga, S., Mochida, M., Saito, T., and Kawamura, K.: In-situ measurement of isoprene in the marine air and surface seawater from the western North Pacific, Atmos. Environ., 36, 6051–6057, 2002.
Meskhidze, N. and Nenes, A.: Phytoplankton and cloudiness in the Southern Ocean, Science, 314, doi:10.1126/science.1131779, 2006.
Middlebrook, A. M., Murphy, D. M., and Thomson, D. S.: Observations of organic material in in-

dividual marine particles at Cape Grim during the First Aerosol Characterization Experiment (ACE-1), J. Geophys. Res., 103, 16475–16483, 1998.
Milne, P. J., Riemer, D. D., Zika, R. G., Brand, L. E.: Measurement of vertical distribution of isoprene in surface seawater, it chemical fate, and its emission from several phytoplankton monocultures, Mar. Chem., 48, 237–244, 1995.
Mishra, D., Narumalani, S., Rundquist, D. and Lawson, M.: Characterizing the vertical diffuse attenuation coefficient for downwelling irradiance in coastal water: Implications for water penetration by high resolution satellite data, J. Photo. & Remote Sensing, 60, 48–64, 2005.
Nenes, A., Charlson, R. J., Facchini, M. C., Kulmala, M., Laaksonen, A., and Seinfeld, J. H.: Can chemical effects on cloud droplet number rival the first indirect effect? Geophys. Res. Lett., 29, doi: -10.1029/2002GL015295, 2002.
Ng, N. L., Kwan, A. J., Surratt, J. D., Chan, A. W. H., Chhabra P. S., Sorooshian A. Pye, H. O. T., Crounse, J. D., Wennberg, P. O., Flagan, R. C., and Seinfeld, J. H.: Secondary organic aerosol (SOA) formation from reaction of isoprene with nitrate radicals (NO_3), Atmos. Chem. Phys., 8, 4117–4140, 2008, http://www.atmos-chem-phys.net/8/4117/2008/.
Novakov, T., Corrigan, C. E., Penner, J. E., Chuang, C. C., Rosario, O., and Mayel Bracero, O. L.: Organic aerosols in the Caribbean trade winds: A natural source?, J. Geophys. Res., 102, 21307–23313, 1997.
O'Dowd, C. D., Hameri, K., Makela, J. M., Pirjola, L., Kulmala, M., Jennings, S. G., Berresheim, H., Hansson, H. C., de Leeuw, G., Kunz, G. J., Allen, A. G., Hewitt, C. N., Jackson, A., Viisanen, Y., and Hoffmann, T.: A dedicated study of new particle formation and fate in the coastal environment (PARFORCE): overview of objectives and initial achievements. J. Geophys. Res., 107, D19, 8108, doi:10.1029/2001JD000555, 2002.
O'Dowd, C. D., Facchini, M. C., Cavalli, F., Ceburnis, D., Mircea, M., Decesari, S., Fuzzi, S., Yoon, Y. J., and Putaud, J. P.: Biogenically driven organic contribution to marine aerosol, Nature, 431, 676–680, 2004.
O'Dowd, C. D. and de Leeuw, G.: Marine aerosol production: a review of the current knowledge, Phil. Trans. R. Soc. A, 365, 1753–1774, 2007.
O'Dowd C. D., Langmann, B., Varghese S., Scannell, C., Ceburnis, D., and Facchini, M. C.: A combined organic-inorganic sea-spray source function, Geophys. Res. Lett., 35, L01801, doi:10.1029/2007GL030331, 2008.
O'Reilly, J. E., Maritorena, S., Mitchell, B. G., Siegel, D. A., Carder, K. L., Garver, S. A., Kahru,

M., and McClain, C.: Ocean color chlorophyll algorithms for SeaWiFS, J. Geophys. Res., 103, C11, 24937–24953, 1998.
Palmer, P. I. and Shaw, S. L.: Quantifying global marine isoprene fluxes using MODIS chlorophyll observations, J. Geophys. Res., 32, L09805, doi:10.1029/2005GL022592, 2005.
Park, R. J., Jacob, D. J., Field, B. D., Yantosca, R. M., and Chin, M.: Natural and transboundary pollution influences on sulfate-nitrate-ammonium aerosols in the United States: Implications for policy, J. Geophys. Res., 109, D15204, doi:10.1029/2003JD004473, 2004.
Pio, C. A., Legrand, M., Oliveira, T., Afonso, J., Santos C., Caseiro, A., Fialho, P., Barata, F., Puxbaum, H., Sanchez-Ochoa, A., Kasper-Giebl, A., Gelencse'r, A., Preunkert, S., and Schock, M.: Climatology of aerosol composition (organic versus inorganic) at nonurban sites on a west-east transect across Europe, J. Geophys. Res., 112, D23, doi:10.1029/2006JD008038, 2007.
Platt, T., Gallegos, C. L., and Harrison, W. G.: Photoinhibition of phytosynthesis in natural assemblages of marine phytoplankton, J. Mar. Res. 38, 687–701, 1980.
Putaud, J. P., Van Dingenen, R., Mangoni, M., et al.: Chemical mass closure and assessment of the origin of the sub-micron aerosol in the marine boundary layer and the free troposphere at Tenerife during ACE-2, Tellus, Ser. B, 52(2), 141–168, 2000.
Richardson, M. I., Toigo, A. D., and Newman, C. E.: PlanetWRF: A general purpose, local to global numerical model for planetary atmospheric and climate dynamics, J. Geophys. Res., 112, E09001, doi:10.1029/2006JE002825, 2007.
Roelofs, G. L.: A GCM study of organic matter in marine aerosol and its potential contribution to cloud drop activation, Atmos. Chem. Phys., 8, 709–719, 2008, http://www.atmos-chem-phys.net/8/709/2008/.
Shaw, G. E.: Bio-controlled thermostasis involving the sulfur cycle, Clim. Change, 5, 297, 1983.
Shaw, S. L., Chisholm, S. W., and Prinn, R. G.: Isoprene production by *Prochlorococcus*, a marine cyanobacterium, and other phytoplankton, Mar. Chem., 80, 227–245, 2003.
Sinha, V., Williams, J., Meyhofer, M., Riebesell, U., Paulino, A. I., and Larsen, A.: Air-sea fluxes of methanol, acetone, acetaldehyde, isoprene and DMS from a Norwegian fjord following a phytoplankton bloom in a mesocosm experiment, Atmos. Chem. Phys., 7, 739–755, 2007, http://www.atmos-chem-phys.net/7/739/2007/.
Smith, M. and Harrison, N.: Marine aerosols concentrations and estimated fluxes over the sea, J. Aerosol Sci., 29, Suppl. 1, S189–S190, 1998.
Tokarczyk, R. and Moore, R.: Production of volatile organohalogens by phytoplankton cultures,

Geophys. Res. Lett., 21, 285–288, 1994.

Turpin, B. J. and Lim, H-J.: Species Contributions to $PM_{2.5}$ Mass Concentrations: Revisiting Common Assumptions for Estimating Organic Mass, Aerosol Sci. Technol., 35(1), 602–610, 2001.

Vaattovaara, P., Huttunen, P. E., Yoon, Y. J., Joutsensaari, J., Lehtinen, K. E. J., O'Dowd, C. D., and Laaksonen, A.: The composition of nucleation and Aitken modes particles during coastal nucleation events: evidence for marine secondary organic contribution, Atmos. Chem. Phys., 6, 4601–4616, 2006, http://www.atmos-chem-phys.net/6/4601/2006/.

Yokouchi, Y., Li, H.-J., Machida, T., Aoki, S., and Akimoto, H.: Isoprene in the marine boundary layer (Southeast Asian Sea, eastern Indian Ocean, and Southern Ocean): Comparison with dimethyl sulfide and bromoform, J. Geophys. Res., 104, 8067–8076, doi:10.1029/1998JD100013, 1999.

Yoon, Y. J., Ceburnis, D., Cavalli, F., et al.: Seasonal characteristics of the physiochemical properties of North Atlantic marine atmospheric aerosols, J. Geophys. Res., 112, D04206, doi:10.1029/2005JD007044, 2007.

Table 1. Global annual total marine emissions of isoprene and OC aerosols.

Global Marine Emissions	Average Estimate	Type	Ref.
Isoprene ($Tg\,C\,yr^{-1}$)	1.2	In-situ	Bonsang et al. (1992)
	0.38	In-situ	Milne et al. (1995)
	0.19	In-situ	Broadgate et al. (1997)
	0.42	In-situ	Baker et al. (2000)
	1.1	In-situ	Matsunaga et al. (2002)
	0.1	Remote Sensing	Palmer and Shaw (2005)
	1.2	In-situ	Sinha et al. (2007)
	0.27	Remote Sensing	Arnold et al. (2008)
	1.68	Modeling	Arnold et al. (2008)
	0.92	Remote Sensing	This work
Sub-micron Primary Organic Carbon ($Tg\,C\,yr^{-1}$)	5.5	Remote Sensing	Spracklen et al. (2008)
	2.5	Remote Sensing	Langmann et al. (2008)
	1.26	Remote Sensing	This work
Super-micron Primary Organic Carbon ($Tg\,C\,yr^{-1}$)	19.01	Remote Sensing	This work
Total Organic Carbon ($Tg\,C\,yr^{-1}$)	8	Remote Sensing	Spracklen et al. (2008)
	75	Modeling	Roelofs (2008)
	20.3	Remote Sensing	This work

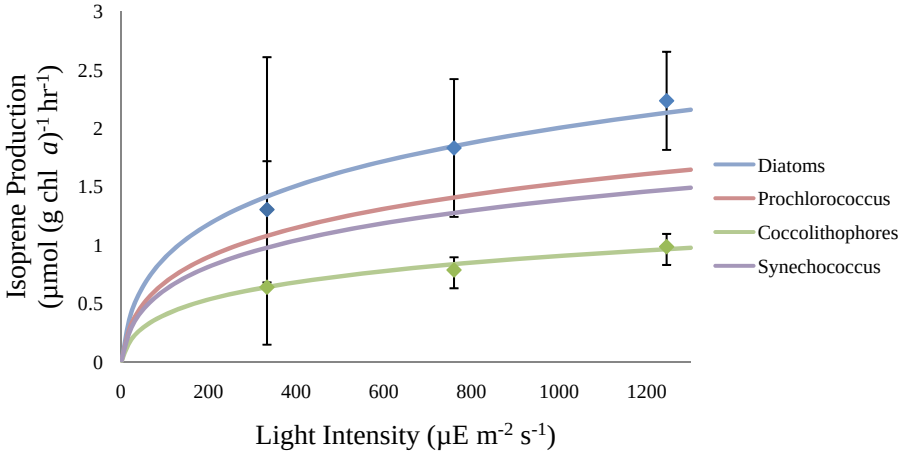

Fig. 1. Isoprene production rates as a function of light intensity for various phytoplankton classes.

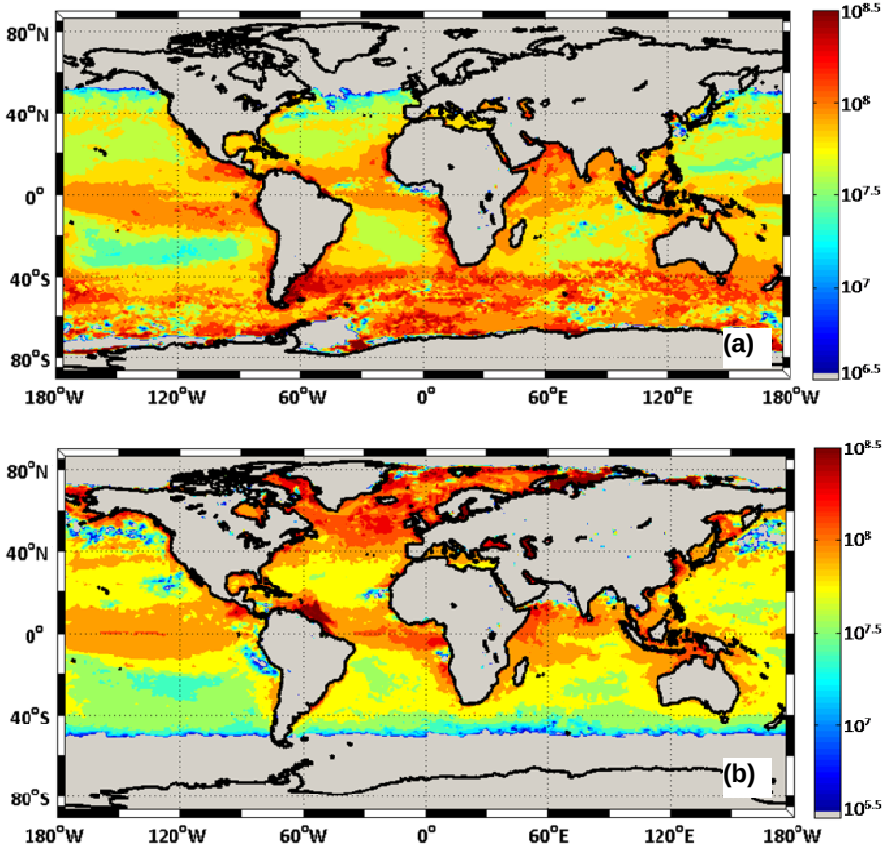

Fig. 2. Monthly-averaged marine isoprene emission rate (molecules cm^{-2} s^{-1}) for **(a)** January and **(b)** July 2001.

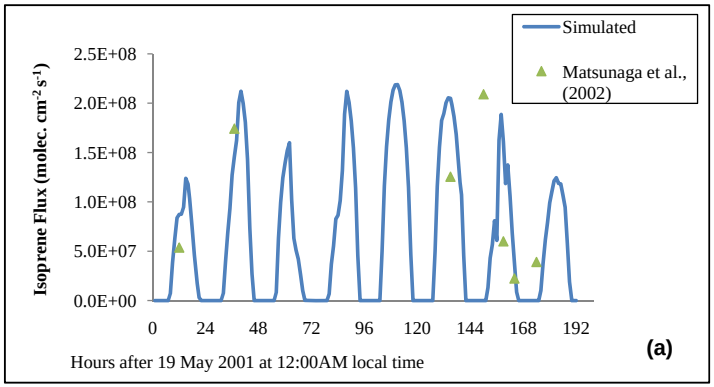

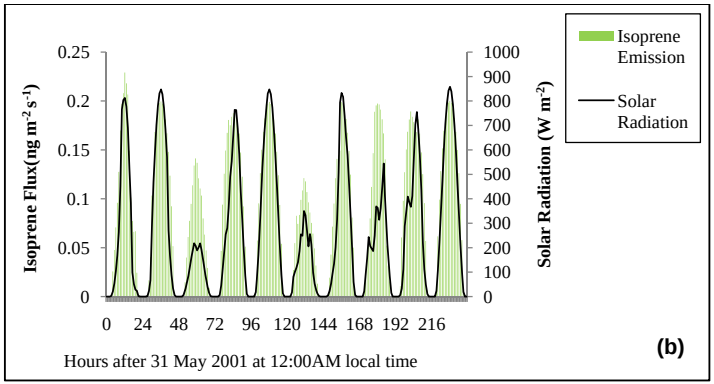

Fig. 3. (a) Comparison of simulated and observed isoprene emissions in the Northern Pacific Ocean along the ship track of Matsunaga et al. (2002); **(b)** Simulated marine isoprene emissions near Raunefjord, Norway in the approximate vicinity of Sinha et al. (2007) measurement site.

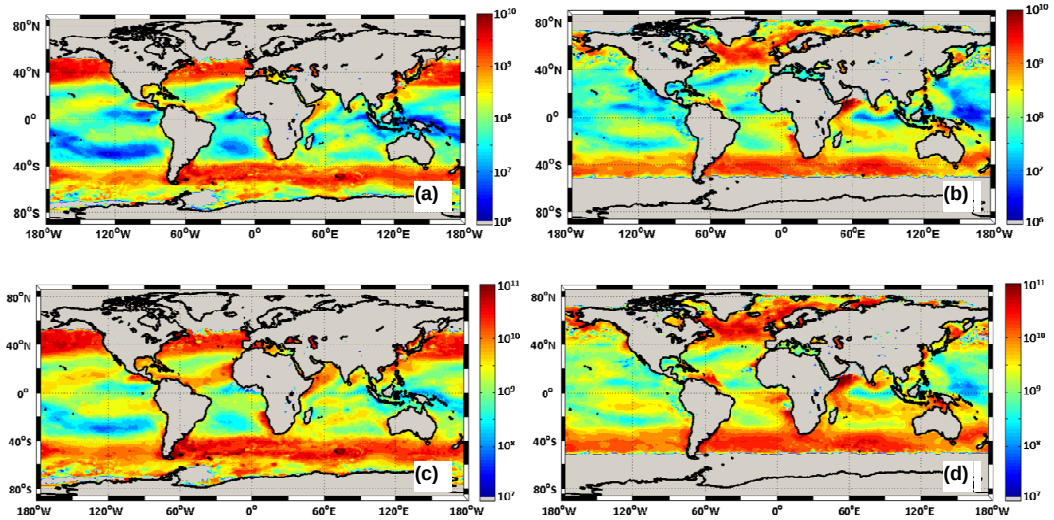

Fig. 4. Monthly-average sub-micron **(a, b)** and super-micron **(c, d)** primary OC emission rate (molecules C cm^{-2} s^{-1}) for January (left column) and July (right column) 2001.

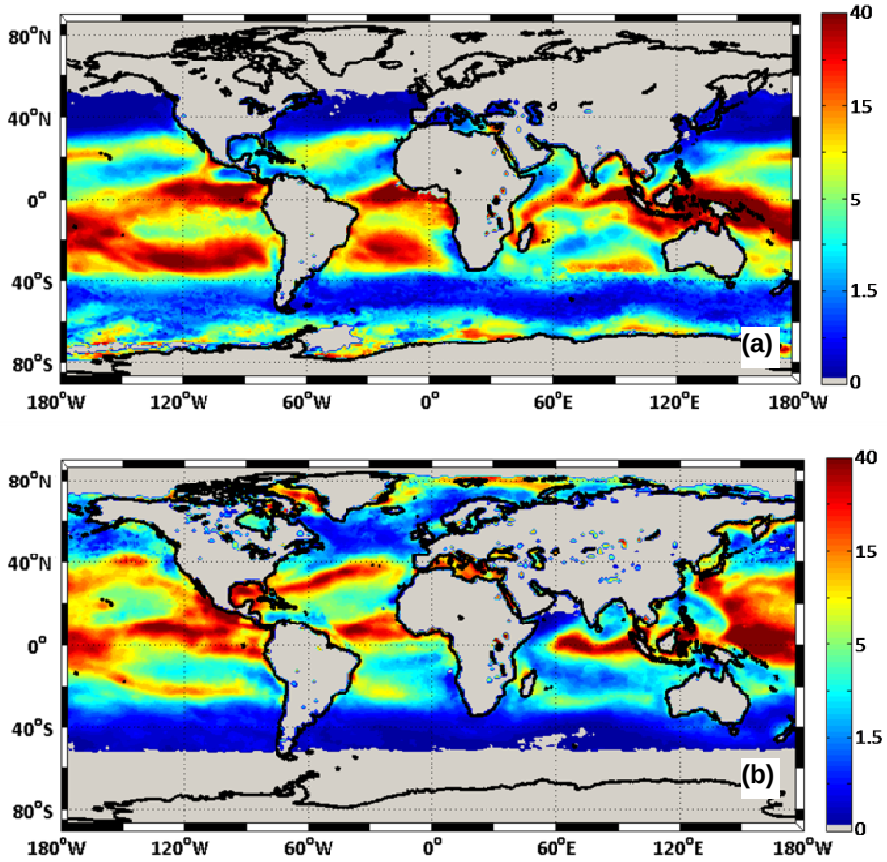

Fig. 5. Monthly-average percent contribution of phytoplankton-derived SOA to total (primary and secondary) sub-micron marine OC emissions for **(a)** January and **(b)** July 2001.

ACPD
9, 2933–2965, 2009

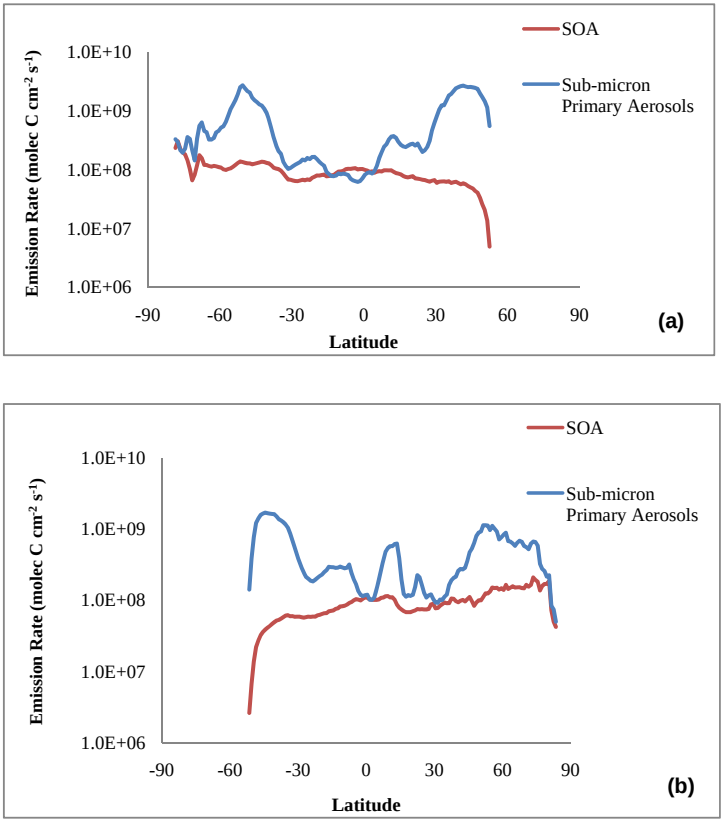

Fig. 6. Monthly-average emission rates of isoprene-derived SOA (red) and sub-micron primary OC aerosols (blue) as a function of latitude for **(a)** January and **(b)** July 2001.

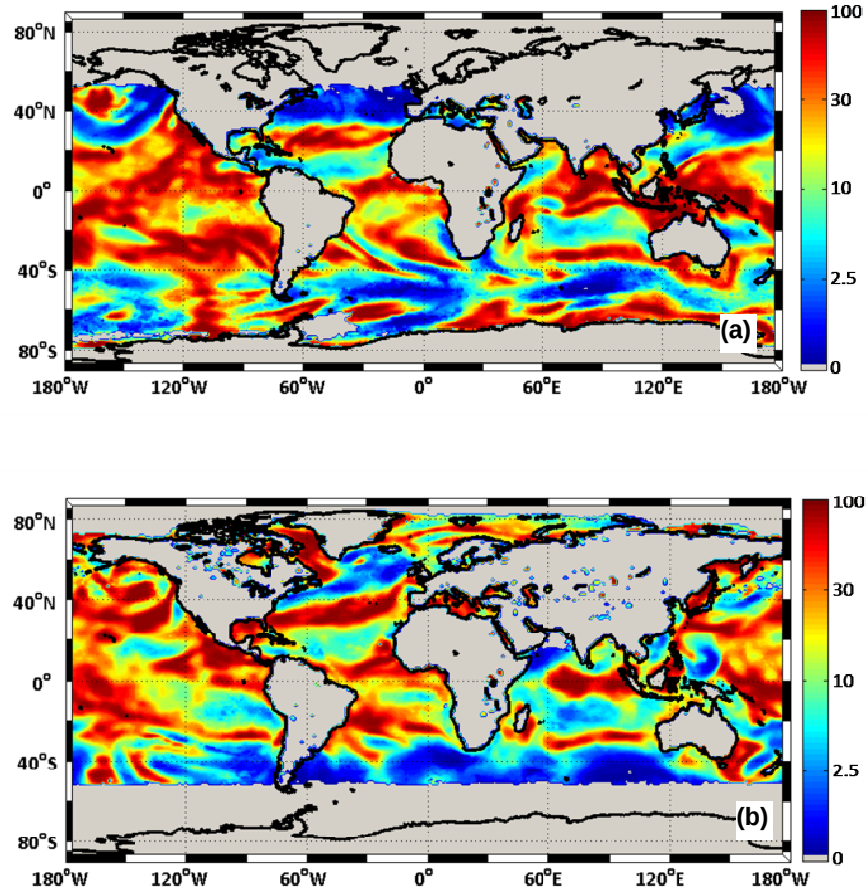

Fig. 7. Percent contribution of 1 h averaged daily maximum phytoplankton-derived SOA to corresponding total (primary and secondary) sub-micron marine OC emissions for **(a)** 1 January and **(b)** 1 July 2001.